



HAL
open science

Impacts of ocean acidification on growth and toxin content of the marine diatoms *Pseudo-nitzschia australis* and *P. fraudulenta*

Nour Ayache, Nina Lundholm, Frederik Gai, Fabienne Herve, Zouher Amzil,
Amandine Caruana

► To cite this version:

Nour Ayache, Nina Lundholm, Frederik Gai, Fabienne Herve, Zouher Amzil, et al.. Impacts of ocean acidification on growth and toxin content of the marine diatoms *Pseudo-nitzschia australis* and *P. fraudulenta*. *Marine Environmental Research*, 2021, 169, 105380 (9p.). 10.1016/j.marenvres.2021.105380 . hal-04203495

HAL Id: hal-04203495

<https://hal.science/hal-04203495>

Submitted on 22 Jul 2024

HAL is a multi-disciplinary open access archive for the deposit and dissemination of scientific research documents, whether they are published or not. The documents may come from teaching and research institutions in France or abroad, or from public or private research centers.

L'archive ouverte pluridisciplinaire **HAL**, est destinée au dépôt et à la diffusion de documents scientifiques de niveau recherche, publiés ou non, émanant des établissements d'enseignement et de recherche français ou étrangers, des laboratoires publics ou privés.



Distributed under a Creative Commons Attribution - NonCommercial 4.0 International License

1 IMPACTS OF OCEAN ACIDIFICATION ON GROWTH AND TOXIN CONTENT OF THE
2 MARINE DIATOMS *PSEUDO-NITZSCHIA AUSTRALIS* AND *P. FRAUDULENTA*

3 **Authors:**

4 Ayache Nour¹, Lundholm Nina², Gai Frederik², Hervé Fabienne¹, Amzil Zouher¹, Caruana
5 Amandine¹

6 ¹Institut Francaise de Recherche pour l'Exploitation de la Mer: Ifremer, Phycotoxin Laboratory,
7 F-44311 Nantes, France

8 ²Natural History Museum of Denmark, University of Copenhagen, Øster Farimagsgade 5, 1307
9 Copenhagen, Denmark

10 **Corresponding author:** Ayache Nour, ayache.nour@gmail.com, Tel: +1 (804) 684-7812,
11 Virginia Institute of Marine Science, PO Box 1346, Gloucester Point, Virginia 23062

12 **Abstract**

13 This paper present the effects of ocean acidification on growth and domoic acid (DA) content of
14 several strains of the toxic *Pseudo-nitzschia australis* and the non-toxic *P. fraudulenta*. Three
15 strains of each species (plus two subclones of *P. australis*) were acclimated and grown in semi-
16 continuous cultures at three pH levels: 8.07, 7.77, and 7.40, in order to simulate changes of
17 seawater pH from present to plausible future levels. Our results showed that lowering pH from
18 current level (8.07) to predicted pH level in 2100 (7.77) did not affect the mean growth rates of
19 some of the *P. australis* strains (FR-PAU-17 and L3-100), but affected other strains either
20 negatively (L3-30) or positively (L3.4). However, the growth rates significantly decreased with
21 pH lowered to 7.40 (by 13% for L3-100, 43% for L3-30 and 16% for IFR-PAU-17 compared to
22 the rates at pH 8.07). In contrast, growth rates of the non-toxic *P. fraudulenta* strains were not
23 affected by pH changing from 8.07 to 7.40.

24 The *P. australis* strains produced DA at all pH levels tested, and the highest particulate DA
25 concentration normalized to cell abundance (pDA) was found at pH 8.07. Total DA content (pDA
26 and dissolved DA) was significantly higher at current pH (8.07) compared to pH (7.77), except for
27 one strain (L 3.4) where no difference was found. At lower pH levels 7.77 - 7.40, total DA
28 content was similar, except for strains IFR-PAU-17 and L3-100 which had the lowest content at
29 the pH 7.77. The diversity in the responses in growth and DA content highlights the inter- and
30 intra-specific variation in *Pseudo-nitzschia* species in response to ocean acidification. When
31 exploring environmental responses of *Pseudo-nitzschia* using cultured cells, not only strain-
32 specific variation but also culturing history should be taken into consideration, as the light levels

33 under which the subclones were cultured, afterwards affected both maximum growth rates and
34 DA content.

35 **Keywords:** amnesic shellfish poisoning; domoic acid; harmful algae; ocean acidification;
36 *Pseudo-nitzschia*

37 **1.1 Introduction**

38 Carbon dioxide (CO₂) concentration in the atmosphere increased from 278 ppm to 400 ppm
39 during the pre-industrial period and is predicted to reach between 800 and 1000 ppm by the end
40 of the 21st century (IPCC, 2014; Le Quéré et al., 2018). As atmospheric CO₂ concentrations
41 continue to increase, the amount of dissolved CO₂ in the ocean will also increase and thus
42 oceanic pH will decrease. Oceanic pH has already decreased by 0.1 unit (from on average 8.21 to
43 8.1) since the beginning of the industrial era, and atmospheric CO₂ is projected to increase and
44 reach about 720-1,020 ppm by the year 2100, which corresponds to a decrease in ocean surface
45 pH by 0.14-0.32 pH units (IPCC, 2014). In addition, coastal and estuarine ecosystems are
46 naturally exposed to pH fluctuations due to upwelling, water depth, tidal currents, residence time,
47 photosynthesis and respiration of phytoplankton (Feely et al., 2008; Middelboe and Hansen,
48 2007). This acidification may have a significant impact on physiology, proliferation and
49 distribution of phytoplankton species in marine ecosystems (Orr et al., 2005). In addition,
50 changes in pH/pCO₂ can have serious consequences for the functioning of marine ecosystems,
51 from direct effects on physiological responses of phytoplankton and zooplankton (Cornwall et al.,
52 2013; Flynn et al., 2015; Kroeker et al., 2013), to more indirect effects on food web and species
53 interactions (Orr et al., 2005). Ocean acidification (OA) may also affect the distribution of

54 phytoplankton, allowing certain species, mainly diatoms, with an efficient carbon concentrating
55 mechanism (CCM), to thrive and dominate the marine ecosystems (Rost et al., 2008; Trimborn et
56 al., 2013). Apart from ocean acidification, enhanced nutrient release from land may also result in
57 enhancing the development of large phytoplankton blooms (of both harmful algal species HABs
58 and non-HABs) and their eventual bacterial decomposition and resultant release of dissolved
59 carbon dioxide and pH decline (Doney, 2010). Climate change-induced ocean acidification and
60 eutrophication may therefore result in a larger increase in HAB bloom biomass, as blooms will
61 initiate at a lower average pH and thus delay the detrimental effects of high pH at bloom
62 maximum (Flynn et al., 2015; Hansen et al., 2007; Lundholm et al., 2004). Several factors are
63 thus in play when discussing the effect of lowered pH/increased DIC availability on HAB
64 species, making it relevant, but not easy, to explore the effect of lowered pH/increased DIC
65 availability on HAB species. Additional impacts by other biotic and abiotic factors like grazers
66 and temperature will also affect the bloom biomass attained. Specific effects of ocean
67 acidification will depend on the physiology of the individual species (Flynn et al., 2015, 2012) as
68 well as any potential physiological variation within a species.

69 The diatom *Pseudo-nitzschia* species are common and abundant members of coastal
70 phytoplankton communities (Malviya et al., 2016; Trainer et al., 2012). Several species of
71 *Pseudo-nitzschia* produce the neurotoxin, domoic acid (DA), which can cause serious ecological,
72 economic, and health-related problems and are responsible for amnesic shellfish poisoning (ASP)
73 in humans world-wide (Bates et al., 2018). In recent decades, numerous reports have linked
74 mortality events of sea birds, fish and sea mammals to the presence of toxic *Pseudo-nitzschia*
75 blooms and the accumulation of high DA concentrations in these organisms (Goldstein et al.,

76 2008; Lefebvre et al., 2012; Scholin et al., 2000). In 2015, a long-lasting geographically
77 extensive bloom of the highly toxic species, *P. australis*, was recorded along the North American
78 west coast causing prolonged closures of shellfish harvesting areas and contributing to the illness
79 and death of seabirds and marine mammals (Di Liberto, 2015; McCabe et al., 2016). As
80 anthropogenic CO₂ emissions continue to increase, it is thus important to understand how growth
81 as well as DA production of *Pseudo-nitzschia* species respond to the ongoing changes in the
82 marine environment (i.e., acidification).

83 In general, acidification has been hypothesized to stimulate primary production of phytoplankton
84 (Riebesell et al., 2007; Rost et al., 2008; Schippers et al., 2004a). Presently, relatively few
85 laboratory studies have examined the effect of lowered pH and increased pCO₂ on the physiology
86 of *Pseudo-nitzschia* species. The findings published show diverging results with respect to
87 growth and DA production in different *Pseudo-nitzschia* species. Studies on *P. fraudulenta* and
88 *P. multiseriis* demonstrate significantly increased growth rates with acidification, and significant
89 increase in DA content with increasing CO₂ concentration especially under nutrient-limiting
90 conditions (Sun et al. 2011 and Tatters et al. 2012). Moreover, Wingert (2017) showed an
91 increase in DA cellular content in a single *P. australis* strain due to acidification, whereas the
92 growth rates in contrast to previous studies were not affected until reaching pH 7.8. In addition,
93 Tatters et al. (2018) found that warming and acidification interactions generally increased the cell
94 normalized DA content in *P. multiseriis* in a mixed, natural assemblage. In recent results of a
95 mesocosm experiment conducted in Gullmar Fjord, Sweden, the authors also observed
96 significantly higher particulate DA contents per litre with elevated pCO₂ (OA), here also

97 associated with macronutrient limitation (Wohlrab et al., 2020). Thus, OA appears to generally
98 increase the production of DA under nutrients limited conditions.

99 The development of high biomass phytoplankton blooms results in lower concentrations of
100 dissolved CO₂ (basification) leading to reduced cellular growth rates in some *Pseudo-nitzschia*
101 species (Lundholm et al., 2004). A decrease in growth rate and simultaneously an increase in DA
102 content was seen in *P. multiseriis* grown at elevated pH levels (pH 8.9) compared to pH 7.9 and
103 8.4 (Lundholm et al., 2004; Trimborn et al., 2008). In contrast, no change in the specific growth
104 rates were observed in *P. multiseriis* and *P. pungens* when maintained under a wide range of pH
105 (from 5 to 9) (Cho et al., 2001). Overall, these apparently contradicting results might be
106 explained by differences in pH levels, differences among *Pseudo-nitzschia* species, as well as
107 different experimental protocols employed (batch and semi-continuous cultures). Most of the
108 existing studies investigating the effect of changing pH on the physiology and DA production by
109 *Pseudo-nitzschia* species used only one strain as representative of a species. Considering the
110 genetic variability of *Pseudo-nitzschia* species (Bates et al., 2018), it is important to study several
111 strains of each species in order to understand the tolerance and toxin production capacity of
112 *Pseudo-nitzschia* species in response to future ocean acidification.

113 In the present study, we examined the effects of lowered pH on growth and DA content in
114 acclimated strains of *P. australis* and *P. fraudulenta* under nutrient replete conditions. The aim
115 was to evaluate the impact of acidification from present (pH 8.07) to probable future levels (pH
116 7.77 and 7.40) in three different strains of two different *Pseudo-nitzschia* species to understand
117 the isolated effects of lowered pH and increased CO₂. *P. australis* and *P. fraudulenta* are

- 118 common and globally widespread species, with *P. australis* being a highly toxic species, and *P.*
- 119 *fraudulenta* a non-toxic or very slightly toxic species.

120 **1.2 Materials and methods**

121 *Cultures and culture conditions*

122 Six monoclonal strains of *Pseudo-nitzschia* were included, three *P. fraudulenta* strains
123 (PNfra167, PNfra169 and IFR-FRA-17) as non-toxic representatives, and three *P. australis*
124 strains (IFR-PAU-17, L3.4 and L3) as toxin-producing strains. Before the experiments, two
125 subclones, L3-30 and L3-100 were established from the same monoclonal culture (L3), which
126 was split and grown at two different culture conditions for at least 3 months: L3-100 was kept at
127 $100 \mu\text{mol photons m}^{-2} \text{s}^{-1}$ cool white light, while L3-30 was kept at $30 \mu\text{mol photons m}^{-2} \text{s}^{-1}$ cool
128 white light (cool-white fluorescent light, Osram, Germany). The six studied strains were isolated
129 from different geographical regions (France and Namibia), (designation and information are
130 given in Table 1. All non-axenic cultures were kept at 15°C in L1 medium (Guillard and
131 Hargraves, 1993) based on autoclaved seawater with a salinity of 32 and a pH value of 8.1. The
132 L1 growth medium was selected to ensure nutrient-replete conditions during the experiment.
133

Table 1: Information on *Pseudo-nitzschia* species and strain designations, sampling location and date, and sources.

Species	Strain	Sampling location	Sampling date	Source
<i>P. australis</i>	IFR-PAU-17	Brest harbor, Brest, France	10/2017	IFREMER, LER-BO, Concarneau, France
<i>P. australis</i>	L3.4	Namibian coasts	12/2016	National Marine Information and Research Centre (NatMIRC), Lüderitz and Swakopmund, Namibia
<i>P. australis</i>	L3	Namibian coasts	12/2016	National Marine Information and Research Centre (NatMIRC), Lüderitz and Swakopmund, Namibia
<i>P. fraudulenta</i>	PNfra 167	Luc sur Mer, English Channel, France	06/2017	UMR BOREA, Normandy university, France
<i>P. fraudulenta</i>	PNfra 169	Luc sur Mer, English Channel, France	06/2017	UMR BOREA, Normandy university, France
<i>P. fraudulenta</i>	IFR-FRA-17	Men Er Roué, Quiberon Bay, France	08/2017	IFREMER, Phycotoxins laboratory, Nantes, France

135 *Experimental set-up*

136 The experiments were carried out at three different pH levels, 8.07 (representing ambient
137 seawater pH level), 7.77 (projected end-of-century seawater pH) and 7.40 (projected pH level by
138 2300) (Caldeira and Wickett, 2003; IPCC, 2014). The L1 medium was acidified to reach the
139 different pH levels 7.40, 7.77 and 8.07 (corresponding to pCO₂ concentrations of 1845, 783 and
140 380 ppm, respectively) by CO₂ bubbling (Air Liquid Denmark A/S. UN 1013 Carbon Dioxide,
141 Class 2, 2A, ADR).

142 The strains of *P. fraudulenta* and *P. australis*, including the two subclones L3-30 and L3-100,
143 were grown in triplicates at the three different pH levels. The cells were acclimated to the
144 different pH treatments for at least 20 generations, and were considered acclimated when growth
145 rates did not vary more than $\pm 0.05 \text{ d}^{-1}$ for at least three consecutive generations at each pH
146 condition (MacIntyre and Cullen, 2005). All cells were grown in triplicate semi-continuous
147 cultures in 65 mL Nunclon polystyrene flasks filled up to capacity with L1 medium of the
148 specific pH value. The cultures were diluted daily, and the dilution rate corresponded
149 approximately to the growth rate, where 60% to 90% d^{-1} of the total culture volume was replaced
150 with an equal volume of pH-specific medium. Daily dilutions were employed to keep the cells at
151 low densities (between 500 and 2000 cell mL^{-1}) in order to avoid pH increases during the
152 experimental period (Hansen et al., 2007; Lundholm et al., 2004). Cultures were kept in
153 suspension by agitation on a plankton wheel (1 rpm) in a temperature-controlled room at 15°C,
154 exposed to a photon flux density of 100 $\mu\text{mol photons m}^{-2} \text{ s}^{-1}$ cool white light following a light:
155 dark cycle of 16: 8 h. The pH level was measured before and after dilution using a WTW pH 340i

156 pH-meter with a SenTix 41 glass electrode, with a sensor detection limit of 0.01. The pH-meter
157 was calibrated daily (2-point calibration) using WTW-pH buffers of pH 7.00 and 10.00.

158 *Growth monitoring*

159 Cell growth was monitored on a daily basis for 14 days by both cell counts (one replicate) and
160 Relative Fluorescence Unit (RFU) measurements (all three replicates). Sub-sampling was carried
161 out at the same time of the day every day. For cell counts, 1 mL samples were fixed with acidic
162 Lugol's solution and a minimum of 400 cells counted using a Nageotte counting chamber and a
163 light microscope Olympus CKX53 at 10× magnification. For RFU measurements, 1 mL was
164 transferred to a quartz cuvette and RFU determined using a Trilogy® laboratory fluorometer
165 (Turner Designs, San Jose, CA, USA). A standard curve for each strain ($r^2 > 0.90$) relating the
166 RFU measurements and the cell counts was used to estimate the cell density for all replicates. For
167 calculation of growth rates, the daily dilutions were taken into consideration. The specific growth
168 rate for the mean value of the triplicates (μ , d^{-1}) was calculated for the last four days of the
169 experiment (when growth rates did not vary more than $\pm 0.05 d^{-1}$) (Guillard, 1973).

170 *Cell volume*

171 For each strain, 50 cells in exponential growth phase were selected and measured using an
172 Olympus BX53 microscope at x100 magnification equipped with an Olympus DP74 digital
173 camera and CellSens imaging software CellSens Entry v1.41. The calculations of cell volume
174 were done at day 0 and 14, and no effect of pH variation on cell volume was observed over the
175 course of the experiment, therefore only the results of the first measurements are shown. Cell
176 volume measurements were calculated for each combination of strain and treatment strain, as

177 mean \pm standard deviation of 50 cells with the assumption that the width and thickness of
178 *Pseudo-nitzschia* cells are similar using the following equation (Lundholm et al., 2004).

179
$$V = \frac{1}{2} a \times b^2$$

180 With a = length, b = width

181 *Nutrient concentrations*

182 Dissolved nutrient concentrations were measured at the beginning and the end of the experiments.
183 Samples (3 \times 24 mL) for inorganic nitrate, phosphate and silicate were passed through
184 polycarbonate 0.2 μ m filters and stored frozen at -20°C immediately after collection, except for
185 silicate samples stored at 4°C. Phosphate and silicate samples were analyzed with a Trilogy®
186 laboratory fluorometer (Turner Designs, San Jose, CA, USA) using standard colorimetric
187 techniques (Hansen and Koroleff, 1999). For analyses of inorganic nitrate, samples were analyzed
188 on an ALPKEM auto-analyzer (Solorzano and Sharp, 1980).

189 *Toxin profile (particulate and dissolved)*

190 On the last day of the experiment, 20 mL of exponentially growing culture was sampled for
191 measuring particulate and dissolved DA fractions. Samples were centrifuged (3000 g, 15 min at
192 4°C) and separated into cell pellet and supernatant. The cell pellet was suspended with 1 mL
193 methanol/water mixture (50/50: v/v) to measure particulate DA content. The extraction was
194 prolonged by 15 min of sonication in an ice-cold bath then centrifuged and filtered (8000 g, 15
195 min, 4°C, 0.2 μ m) to recover the supernatant and stored at -80°C for later analyses (Calu, 2011).
196 DA content in the dissolved fraction was extracted by solid phase extraction (SPE) using Agilent

197 Bond Elut 200 mg C₁₈ cartridges (Ayache et al., 2019). The SPE column was conditioned with 10
198 mL methanol followed by 10 mL high purity water. The sample was acidified with 20% aqueous
199 formic acid (200 µL) then passed through the SPE column. The cartridge was rinsed with 10 mL
200 of 0.2% aqueous formic acid then dried for 1 minute. DA was eluted with 1.5 mL of
201 methanol/water (50/50: v/v) into a glass vial and stored at -80 °C for later analysis.

202 DA analyses were performed using Ultra-Fast Liquid Chromatography (UFLC, Shimadzu)
203 coupled to an ABSciex API 4000 Q-Trap (triple quadrupole mass spectrometer) (Ayache et al.,
204 2019). The chromatographic separation was carried out on a Kinetex C₁₈ column (150 × 2.1 mm,
205 2.6 µm, Phenomenex) equipped with a pre-column. A certified DA standard (CNRC, Halifax,
206 Canada) was used for external calibration range in order to quantify DA. The limit of detection
207 (LOD) and limit of quantification (LOQ) were respectively 0.1 and 0.25 ng mL⁻¹. The particulate
208 (pDA) and dissolved DA (dDA) contents were expressed on a per cell basis (pg cell⁻¹). Total DA
209 (tDA) is calculated by addition of pDA and dDA.

210 *Dissolved inorganic carbon*

211 The concentration of dissolved inorganic carbon (DIC) in the medium in all three pH treatments
212 was measured in triplicates at the end of the experiment. DIC samples (2 × 12 mL) were
213 preserved with mercuric chloride and stored in airtight borosilicate flasks without headspace (to
214 avoid CO₂ leaking out of the water phase) in the dark at 4°C until measurements. DIC
215 concentrations were measured on 1 ml subsamples using an infrared gas analyzer (ADC 225
216 Mk3, Analytic Development Co. Ltd., Hoddesdon, England) as described in detail elsewhere
217 (Nielsen et al., 2007). The carbon speciation (HCO₃⁻, CO₃²⁻ and CO₂* [*includes H₂CO₃ and

218 CO₂] was calculated from pH and DIC concentration at a temperature of 16°C and salinity 32.
219 Calculations were made using the CO2SYS program and the following available inputs: set of
220 constants: K1, K2 from Mehrbach et al. (1973) refit by Dickson & Millero (1987); KHSO₄:
221 Dickson; pH scale: seawater (SW) scale (mol kg⁻¹ SW) (Lewis and Wallace, 1998).

222 *Statistical analyses*

223 The experiments were carried out in triplicate and the data presented as mean values ± standard
224 deviation (SD). Statistical differences among growth rates, cell volumes, nutrients concentrations
225 and DA content at the different pH levels were determined using a one-way analysis of variance
226 (ANOVA). A pair-wise Tukey HSD multiple comparisons test was performed to identify
227 differences between pH treatments. All data was normally distributed, as determined by the
228 Shapiro-Wilk test, thus permitting the use of parametric statistical analyses. The level of
229 significance (α) was set to 0.05 for all statistical tests.

230 **1.3 Results**

231 *1.3.1 Effect of pH variation on growth and cell volume*

232 The mean growth rates of the *Pseudo-nitzschia australis* strains (including the two clones L3-30
233 and L3-100) were significantly affected by pH (Fig. 1A, Table S1). In strain L3-30, the mean
234 growth rate was significantly higher at pH 8.07 (2.47 d⁻¹) compared to pH 7.77 (2.33 d⁻¹) and pH
235 7.40 (1.72 d⁻¹) ($p < 0.01$). The highest mean growth rates for strains IFR-PAU-17 and L3-100
236 occurred at pH 7.77, which were not significantly different from their respective mean growth
237 rates at pH 8.07 ($p > 0.05$) (Fig. 1A, Table S1). Growth rates decreased significantly for these
238 three strains (IFR-PAU-17, L3-100 and L 3-30) when pH declined to pH 7.40 ($p < 0.001$) (Fig.

239 1A). Whereas for strain L3.4, a significantly higher growth rate ($p < 0.01$) was observed at pH
240 7.77 in comparison to pH 8.07 (1.65 and 1.43 d^{-1} , respectively), and a continued increase,
241 although not significant ($p > 0.05$), was observed between pH 7.77 and 7.40 (1.72 d^{-1}) (Fig. 1A,
242 Table S1).

243 When comparing growth rates among strains in *P. australis*, the overall highest growth rate was
244 observed for strain L3-30 at pH 8.07 (2.47 d^{-1}), which was 1.4-fold higher than in strain L3-100
245 (1.77 d^{-1}), followed by the strain IFR-PAU-17 grown at the same pH (1.67 d^{-1}) ($p < 0.001$) (Fig.
246 1A, Table S1). The overall lowest growth rate was obtained in strain L3.4 at the same pH, 8.07
247 (1.43 d^{-1}) (Fig. 1A). Hence, intraspecific variation in growth rates of *P. australis* at similar pH
248 conditions was considerable, exhibiting a maximum variation spanning from 1.43 to 2.47 d^{-1} at
249 pH 8.07.

250 In contrast to *P. australis*, the mean growth rates of the three *P. fraudulentata* strains were not
251 significantly affected by the pH level ($p > 0.05$). The growth rates ranged between 1.76 and 1.82
252 d^{-1} in strain IFR-FRA-17, between 2.02 and 2.00 d^{-1} in strain PNfra167 and between 1.79 d^{-1} and
253 1.72 d^{-1} in strain PNfra169, grown at pH 8.07 and 7.77, respectively. All *P. fraudulentata* strains
254 showed lower, but not significantly lower, growth rates at the lowest pH (7.40) (1.72, 1.90 and
255 1.64 d^{-1} for IFR-FRA-17, PNfra167 and PNfra169, respectively) compared to the two other pH
256 levels ($p > 0.05$) (Fig. 1B, Table S1). In *P. fraudulentata*, the highest growth rate was obtained in
257 PNfra167 at pH 8.07 (2.02 d^{-1}) and the lowest in strain PNfra167 at pH 7.40 (1.64 d^{-1}) (Fig. 1B,
258 Table S1). Intraspecific variation in growth rates at the same pH was hence considerably smaller
259 in *P. fraudulentata* than in *P. australis* varying maximally from 1.76 to 2.02 d^{-1} and from 1.43 to
260 2.47 d^{-1} for *P. fraudulentata* and *P. australis* strains, respectively at pH 8.07 (Table S1). In spite of

261 differences among strains, an overall significant negative effect of OA was found on the growth
 262 rate of all *P. australis* strains with pH decreasing from 8.07 to 7.40 ($p < 0.005$) and from pH 7.77
 263 to 7.40 ($p < 0.05$), whereas, no significant effect of pH changes was detected on *P. fraudulenta*
 264 strains.

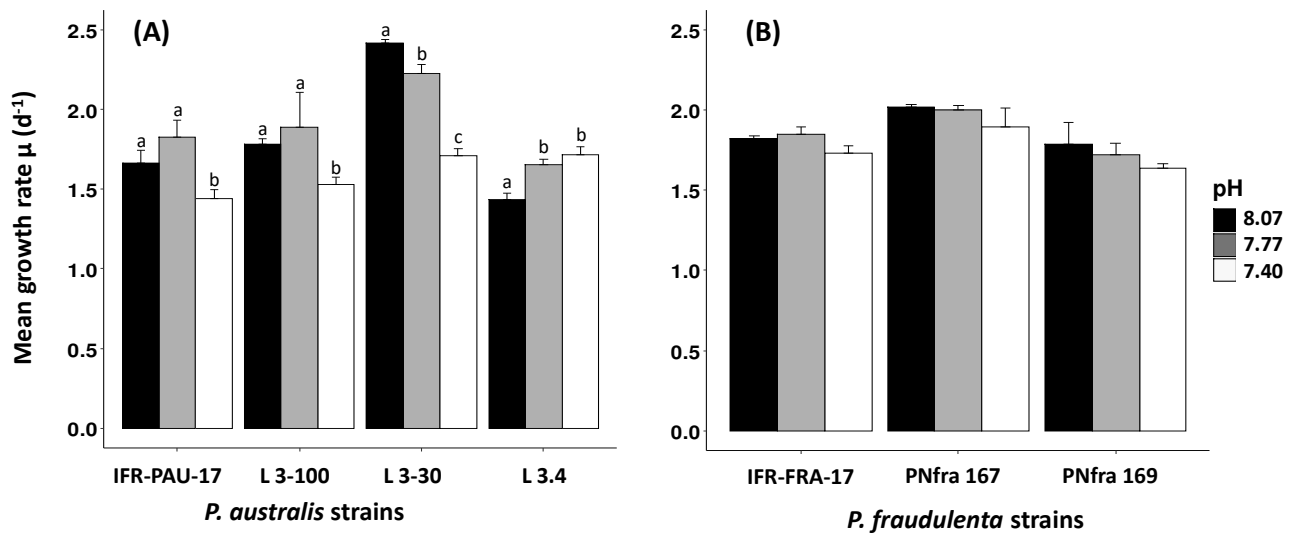


Figure 1: Mean growth rate (d^{-1}) for (A) *P. australis* strains (IFR-PAU-17, L 3.4, L 3-30 and L 3-100) and (B) *P. fraudulenta* strains (IFR-FRA-17, PNfra 167 and PNfra 169) acclimated at three different pH levels (pH= 8.07, 7.77 and 7.40). Error bars represent \pm SD, $n=3$. For each strain, pH treatments with different superscript letters were significantly different.

265 No effect of pH on the cell volume was observed for all the studied strains. For the *P. australis*
266 strains, the mean cell volumes ranged between 629 μm^3 and 1642 μm^3 and between 660 μm^3 and
267 1179 μm^3 for the *P. fraudulenta* strains (Fig. 2A and B). The strains of the two species therefore
268 have similar cell volumes. In *P. australis*, the highest cell volume was observed in strain L3-30
269 (1642 μm^3) which differed significantly ($p < 0.05$) from strains IFR-PAU-17 and L3-100 (1241
270 and 1112 μm^3 , respectively). The lowest cell volume, however, was obtained in L3.4 (627 μm^3),
271 which was significantly lower ($p < 0.05$) than all the other *P. australis* strains (Fig. 2A). The cell
272 volumes of the subclones L3-30 and L3-100 were affected by the culturing history ($p < 0.001$),
273 because the subclone grown at the highest light intensity (L3-100) had a 32% smaller cell volume
274 compared to L3-30 (Fig. 2A). In *P. fraudulenta*, the highest cell volume, obtained in strain IFR-
275 FRA-17 (1179 μm^3), differed significantly from the two other strains PNfra167 and PNfra169,
276 which were not significantly different from each other (696 and 660 μm^3 , respectively) ($p > 0.05$)
277 (Fig. 2B).

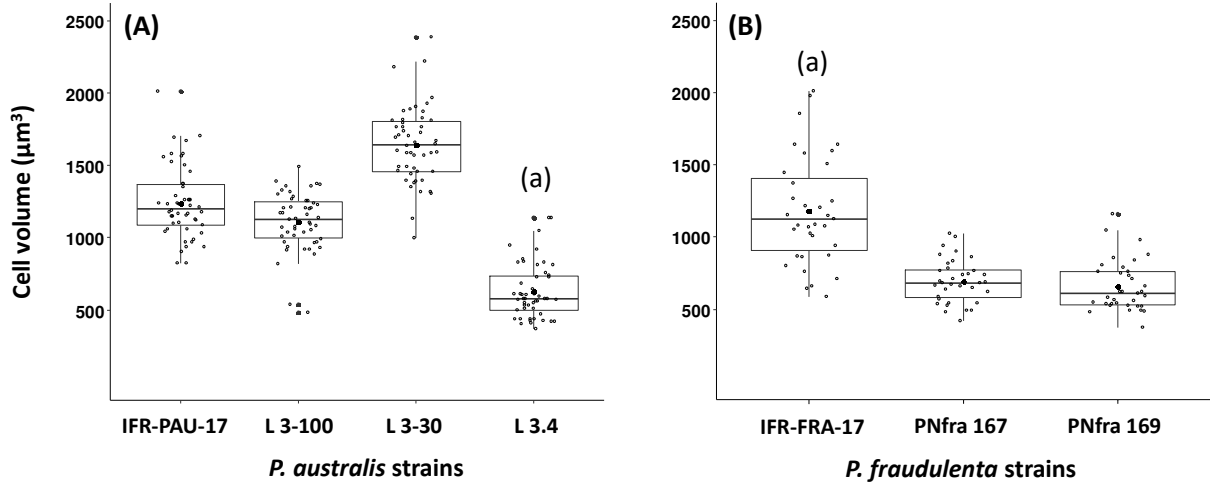


Figure 2: Mean cell volume (μm^3) for (A) *P. australis* strains (IFR-PAU-17, L 3.4, L 3-30 and L 3-100) and (B) *P. fraudulenta* strains (IFR-FRA-17, PNfra 167 and PNfra 169). Error bars represent \pm SD, $n=50$.

(a) Significant difference existed among the mean cell volume of one strain compared to the other strains of the same species ($p < 0.001$).

279 1.3.2 Measurements of pH, dissolved nutrients and inorganic carbon (DIC) content

280 The pH in all the experimental treatments fluctuated minimally ($< \pm 0.02$ units) from the
281 designated pH levels of 8.07, 7.77 and 7.40 throughout the experimental period (Fig. 3).

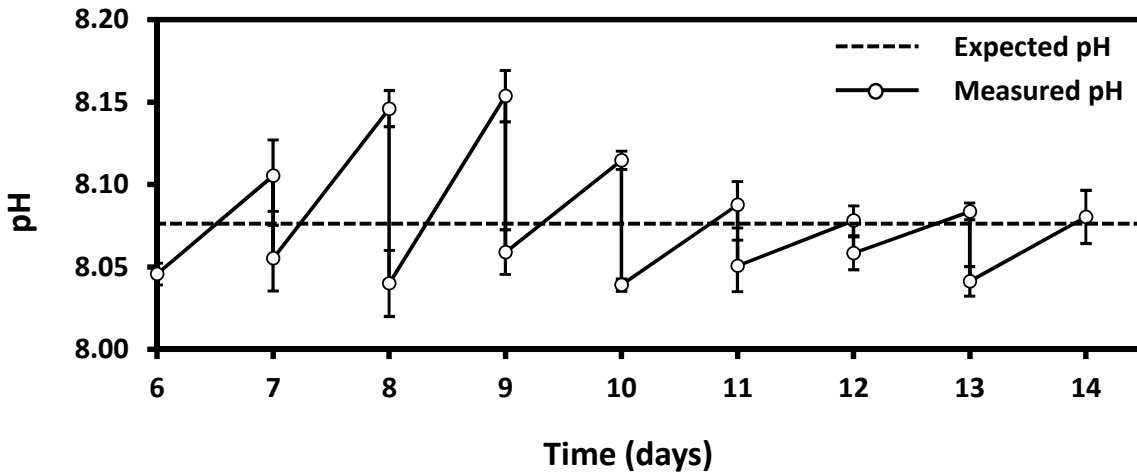


Figure 3: Example of pH adjustments for the culture of *P. australis* IFR-PAU-17 under the pH treatment 8.07. The first days represent the acclimation period and are not included in the results. Error bars represent \pm SD, $n=3$.

282

283 Dissolved nitrogen (N), phosphate (P) and silicate (Si) concentrations were measured in the L1
284 medium prepared for the experiments, and on the last day of sampling. The mean nutrient
285 concentration in all strains acclimated to the different pH levels were equal to 664 μ M dissolved
286 N, 33.5 μ M dissolved P and 144.8 μ M dissolved Si (Table S2), and hence none of the strains
287 were nutrient-limited at any of the pH levels.

288 The DIC concentrations measured in the *P. australis* strains ranged between 1924 and 2104 μmol
289 L^{-1} , and between 2016 and 2173 $\mu\text{mol L}^{-1}$ for *P. fraudulenta* strains for all pH treatments (Table
290 S3). As expected, the concentrations of HCO_3^- , CO_3^{2-} and CO_2 were significantly different among
291 the pH treatments ($p < 0.05$) (Table S3). In all pH treatments, the carbon speciation of DIC was
292 dominated by bicarbonate ion (HCO_3^-). The concentrations of HCO_3^- (91% to 95%) and CO_2 (1%
293 to 3%) increased with decreasing pH from pH 8.07 to pH 7.40, respectively, whereas the
294 concentration of CO_3^{2-} decreased (8% to 2%) (Table S3).

295 *1.3.3 Effect of pH variation on toxin content*

296 No particulate (pDA) or dissolved domoic acid (dDA) was detected in any of the *P. fraudulenta*
297 strains at a detection limit of 0.1 ng mL^{-1} . The *P. australis* strains confirmed their capability for
298 DA production at all three pH levels (pDA and dDA) (Fig. 4A and B, Table S4). Despite the
299 differences in biovolume among the *P. australis* strains, pDA and dDA contents showed the same
300 trend when expressed per cell and per volume, therefore only content per cell are presented
301 below.

302 For *P. australis* strain IFR-PAU-17 and the two clones L3-100 and L3-30, particulate DA content
303 was significantly higher ($p < 0.001$) at pH 8.07 relative to pH 7.77 (Fig. 4A), whereas pDA
304 content remained unchanged in strain L3.4 ($p > 0.05$). At the lowest pH 7.40, all strains showed
305 relatively constant cellular DA content relative to pH 7.77 ($p > 0.05$), except for strain IFR-PAU-
306 17. The latter's pDA was significantly higher at pH 7.40 (1.23 pg cell^{-1}) than at pH 7.77 (0.25 pg
307 cell^{-1}) but still lower than pH 8.07 (2.49 pg cell^{-1}) ($p < 0.01$). All strains thus showed lower or
308 unchanged particulate DA content (except for strain IFR-PAU-17) with pH decreasing from 8.07

309 to 7.40 (Table S4). The highest pDA content was detected in IFR-PAU-17 at pH 8.07 (2.49 pg
 310 cell⁻¹). The two clones L3-30 and L3-100 showed similar patterns for pDA contents at the three
 311 pH treatments (Fig. 4A). The highest pDA content in clone L3-100 (1.64 pg cell⁻¹ at pH 8.07),
 312 was significantly higher (4-fold) than the pDA content of the clone L3-30 acclimated at the same
 313 pH (0.37 pg cell⁻¹). Overall, the lowest pDA content was obtained in strain L3.4 and it did not
 314 differ significantly ($p > 0.05$) among the three pH levels tested (ranging between 0.06 and 0.07 pg
 315 cell⁻¹ at pH 7.40, 7.77 and 8.07) (Fig. 4A, Table S4).

316

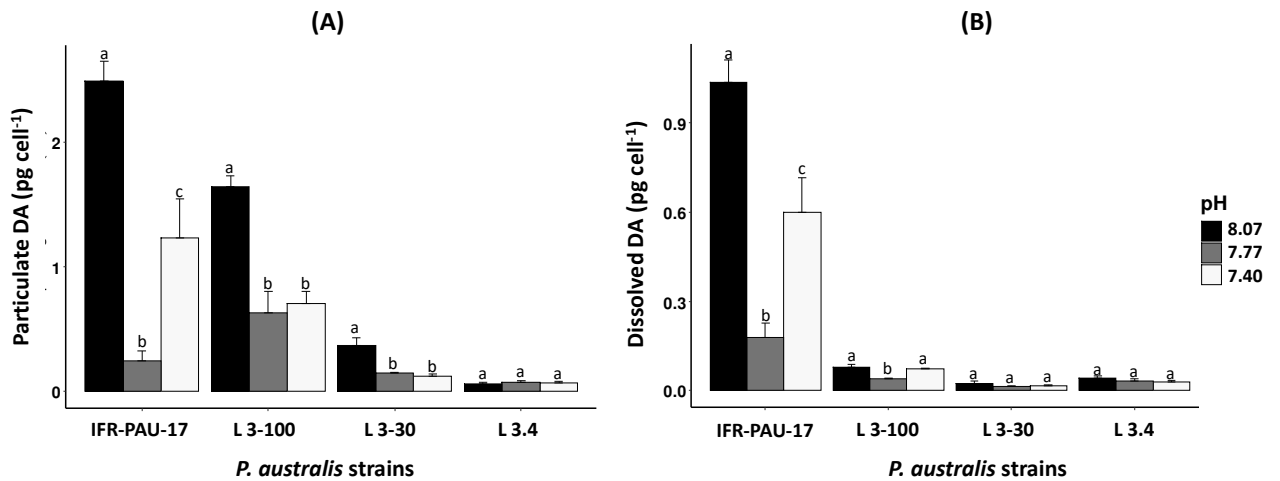


Figure 4: Particulate (A) and dissolved (B) DA contents (pg cell⁻¹) for *P. australis* strains (IFR-PAU-17, L 3.4, L 3-30 and L 3-100) acclimated at three different pH levels (pH= 8.07, 7.77 and 7.40). Data are means \pm SD, n=3. For each strain, pH treatments with different superscript letters were significantly different.

317 Similar to pDA, the highest dDA content for all *P. australis* strains was detected at the highest
318 pH treatment 8.07 (Fig. 4B). At this pH, dDA content was significantly higher ($p < 0.001$) in
319 strain IFR-PAU-17 ($1.04 \text{ pg cell}^{-1}$) compared to the three other strains L3-100 (13-fold), L3.4
320 (26-fold) and L3-30 (52-fold) at the same pH (Fig. 4B, Table S1). In strains IFR-PAU-17 and L3-
321 100, dDA content was significantly higher at pH 8.07 ($p < 0.001$) compared to the pH level 7.77,
322 whereas in the other two strains there was no significant difference (Fig. 4B). In strain IFR-PAU-
323 17, dDA was significantly higher at pH 7.40 ($0.60 \text{ pg cell}^{-1}$) in comparison with pH 7.77 (0.18 pg
324 cell^{-1}) ($p > 0.05$) (Fig. 4B). A similar, but not significant, pattern was seen for strain L3-100 with
325 2-fold increasing dDA levels from pH 7.77 to pH 7.40 (Fig. 4B, Table S4). Whereas strains L3.4
326 and L3-30 did not show any significant differences in dDA content among any of the three pH
327 levels ($p > 0.05$) (Fig. 4B).

328 The overall variations in total cellular content of DA (tDA) were similar to variations in pDA.
329 The highest tDA content was obtained at pH 8.07 for most of the *P. australis* strains IFR-PAU-17
330 ($3.53 \pm 0.23 \text{ pg cell}^{-1}$), L3-100 ($1.72 \pm 0.10 \text{ pg cell}^{-1}$) and L3-30 ($0.39 \pm 0.07 \text{ pg cell}^{-1}$). At pH
331 8.07, strain IFR-PAU-17 produced the highest amount of total DA ($3.53 \pm 0.23 \text{ pg cell}^{-1}$) (Table
332 S4), while the lowest tDA content was obtained in strain L3.4 ($0.10 \pm 0.02 \text{ pg cell}^{-1}$) (Table S4).
333 Interestingly, in strains L3.4 and IFR-PAU-17, dissolved DA as a percentage of total DA ranged
334 from 30%-40% for the two species at all three pH levels, whereas the dDA fraction in strains L3-
335 30 and L3-100 represented maximum 7 % of the tDA content at all pH levels with the exception
336 of strain L3-30 at pH 7.40 where the dDA fraction represented 13 % of the total DA content (Fig.
337 5).

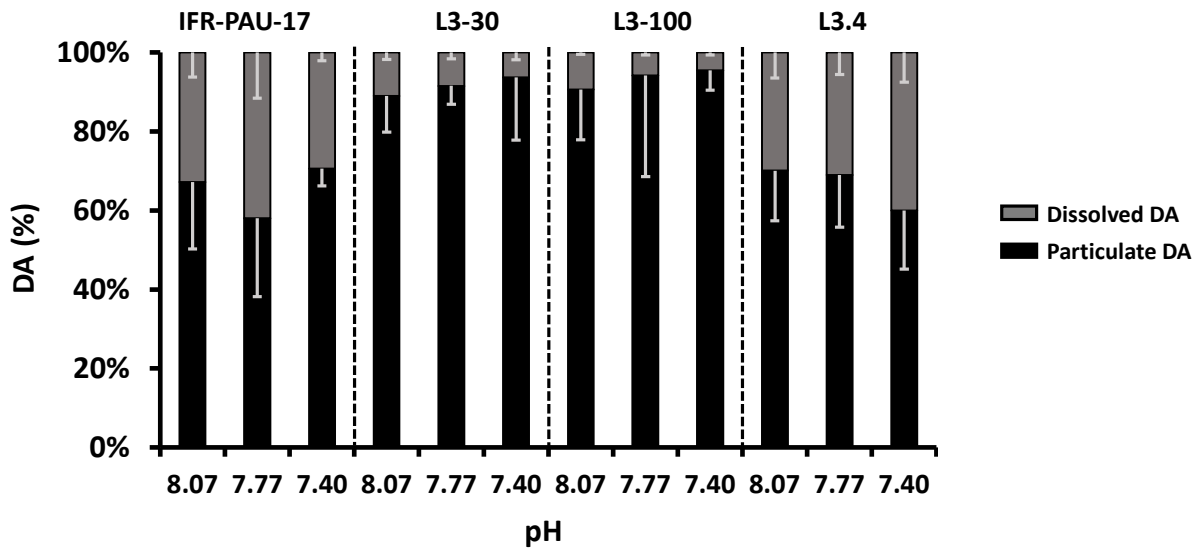


Figure 5: Particulate and dissolved DA expressed as a percentage of total DA at the different pH levels: 8.07, 7.77 and 7.40 in *P. australis* strains (IFR-PAU-17, L 3.4, L 3-30 and L 3-100)

Data are means \pm SD, n=3.

339 **1.4 Discussion**

340 *1.4.1 Effect of pH variation on growth rate*

341 The mean growth rates for two *P. australis* strains (IFR-PAU-17 and L 3-100) did not vary
342 between pH levels 8.07 and 7.77. However, their mean growth rates at pH 7.40 were 11-30% and
343 19-26% lower compared to what was measured at pH of 8.07 and 7.77, respectively. By contrast,
344 lowering pH from current level (8.07) to predicted pH level in 2100 (7.77) affected other strains
345 either negatively (L3-30) or positively (L3.4). However, there was no statistical variation in
346 growth rate of the three non-toxic *P. fraudulenta* strains grown at pH equal to 8.07, 7.77 and
347 7.40. Apparently contrasting results were reported for the polar species *Pseudo-nitzschia*
348 *subcurvata*, where growth rates increased significantly with increased CO₂/lowered pH levels
349 from 205ppm ~ pH 8.31 to 425 ppm ~ pH 8.02 (Zhu et al. (2017). These experiments were,
350 however, performed mainly at CO₂ concentrations lower than current atmospheric levels of ~400
351 ppm (pH 8.05) and did not explore scenarios of ocean acidification. Similar to our findings,
352 Wingert et al. (2017) reported a decrease in growth rate for an *P. australis* strain cultured at pH
353 7.8 (0.95 d⁻¹) (ca. 30 % decrease) in comparison with the three higher pH treatments pH 8.1, 8.0
354 and 7.9 ($\mu = 1.33, 1.26$ and 1.30 d⁻¹, respectively). Moreover, Hancock et al. (2018) and Davidson
355 et al. (2016) found negative effects of high CO₂/low pH on the abundance of *P. subcurvata* in
356 natural communities, as well as in a mixed Antarctic microbial assemblage, respectively. Other
357 studies, including most of our results, hence show a lower growth rate in *Pseudo-nitzschia* with
358 ocean acidification. A possible explanation for the decrease in growth rates with decreasing pH
359 (and increasing in H⁺ ions) may be linked to potentially more energy spent on maintaining pH
360 homeostasis necessary for cell functioning at the expense of growth in these strains (Beardal and

361 Raven, 2004; Riebesell, 2004; Berge et al.2010), and deviations from optimum intracellular pH of
362 cells may directly affect physiological processes such as enzyme activity, protein function,
363 nutrient uptake (Gattuso and Hansson, 2009; Graneli and Haraldsson, 1993; McMinn et al.,
364 2014).

365 In contrast to the above-mentioned results, a single strain of *P. australis*, L3.4, showed an overall
366 positive effect on growth rate of lower pH conditions (7.40) compared to higher pH (8.07) in the
367 present study (Fig. 1A). Similarly, based on figure-derived rates, a relative increase in growth
368 rates (from 0.4 to 0.7 d⁻¹) were found with increasing pCO₂ (from 220 ppm to 730 ppm
369 corresponding to approximately pH 8.19 and 7.96, respectively) for a *P. multiseriis* strain
370 maintained under nutrient-replete conditions (Sun et al., 2011). In addition, in *P. fraudulenta*
371 nutrient-replete cultures, Tatters et al. (2012) also reported a significant progressive increase in
372 growth rates with increasing pCO₂ levels (an increase of 48% and 66% relative to the 200 ppm ~
373 pH 8.43, 360 ~ pH 8.22 and 765 ppm ~ pH 7.95, respectively). Several studies thus also report
374 positive effects on growth rates in *Pseudo-nitzschia* due to experimental OA. Increased
375 concentrations of atmospheric CO₂ from current levels to 700 ppm (~ pH 7.81) has been
376 suggested to generally increase the growth of marine phytoplankton by 40% (Schippers et al.,
377 2004b), especially for species relying on CO₂ or HCO₃⁻ uptake (Hein and Sand-Jensen, 1997;
378 Riebesell et al., 2007). In *Pseudo-nitzschia* species, *P. multiseriis* has been shown to rely almost
379 equally on CO₂ or HCO₃⁻ uptake (Trimborn et al. 2008); nothing is known for other *Pseudo-*
380 *nitzschia* species. Most phytoplankton species have highly regulated carbon concentrating
381 mechanisms (CCMs), that might allow them to avoid CO₂ limitation and support their
382 photosynthesis productivity at low pCO₂ (high pH) levels (Reinfelder, 2011; Sobrinho et al.,

383 2017; Trimborn et al., 2013). At low pH levels, however, relatively more carbon is available as
384 CO₂ and HCO₃⁻ and it is not likely that *Pseudo-nitzschia* suffer carbon-limitation. Operating and
385 maintaining CCMs requires cellular energy (ATP), therefore, cells grown at lower pH might use
386 less energy for CCMs and thus have higher growth rates (Hopkinson et al., 2010; Hutchins et al.,
387 2009).

388 The contrasting results observed in our experiment between the tested *P. australis* strains
389 illustrate the need to include multiple strains, and to perform studies on populations (natural or
390 artificial) to understand responses of individual species, and communities, to future OA. For
391 comparison among studies, differences in experimental set-up further complicates conclusions,
392 but even with our relatively restricted number of strains, we saw contrasting results in growth
393 response to OA. This may seem logical, but none the less, deductions based on single strains are
394 often made when considering effects of relevance for HAB blooms or ecosystem effects.

395 1.4.2 Effect of culturing on growth rate physiology

396 The two subclones with a different culturing history regarding light intensity had different cell
397 volumes. The differences observed in subclone-specific may be explained by the fact that the
398 growth of unicellular microalgae is inversely proportional to their cell size (Banse, 1976). This
399 was also observed in the present study. The strains with the lowest growth rate, L3-30, showed a
400 rather a higher cell volume compared to small-sized subclone, L3-100, the cell volume of which
401 was ca. 32 % smaller (Fig. 2A). Combining the facts that 1) at higher light intensity, *Pseudo-*
402 *nitzschia* cells have been shown to accelerate their growth rate (Auro and Cochlan, 2013; Pan et
403 al., 1996; Thorel et al., 2014), and 2) that diatom cells are known to gradually decrease in overall

404 cell size during vegetative reproduction e.g. (Mann, 1988), explains why the subclone grown at
405 high light generally had a smaller cell volume. Therefore, the decrease in growth rate in L3-100
406 compared to L3-30 may be due to differences in the physiological state of the cells (they are
407 physiologically “older”), as subclone L3-100 was subjected to accelerated division conditions
408 (high light) compared to L3-30 maintained at low light.

409 *1.4.3 Effect of pH variation on particulate and dissolved DA content*

410 As expected, DA was produced by the potentially toxic strains of *P. australis*, while no DA
411 production was found in the strains of *P. fraudulenta*.

412 The particulate DA content decreased significantly in most of the toxic *P. australis* strains (IFR-
413 PAU-17, L3-30 and L3-100) with pH decreasing from 8.07 to 7.77, and was most pronounced for
414 strain IFR-PAU-17 where the decrease in particulate DA content was almost 10-fold (Fig. 5). In
415 contrast the last strain, L3.4, showed no significant change in particulate DA content.

416 Only few studies have explored effects of ocean acidification i.e. lowered pH on DA production,
417 having used either a single strain of *Pseudo-nitzschia* or a mixed natural community (Sun et al.,
418 2011; Tatters et al., 2018, 2012; Wingert, 2017; Wohlrab et al., 2020). All studies reported that
419 projected future 2100 levels (pH 7.8-7.9) compared with present day CO₂ /pH levels (pH c. 8.1)
420 resulted in higher DA content, i.e. the opposite result of the present study. Sun et al. (2011) and
421 Tatters et al. (2012) observed an increase in total DA content in treatments combining high
422 pCO₂/low pH levels (2100 CO₂ levels 800 ppm ~ pH 7.95 compared to current concentrations
423 360 ppm ~ pH 8.22) with nutrient-limited growth conditions. The authors suggested that higher
424 pCO₂ concentrations induced DA production as a consequence of an excess carbon supply
425 together with phosphorus and silicon-limited treatments for both *P. multiseriata* and *P.*

426 *fraudulenta* species, respectively. But under P-replete conditions, Sun et. al. (2011) showed that
427 although total DA did increase by 2-3 fold, the actual DA concentrations were 30-50-fold lower
428 than at similar pH conditions under nutrient-deplete conditions. This is very similar to Wingert et
429 al. (2017) who also only found an increase in total DA content in stationary phase nutrient-
430 limited *P. australis* cells (3 to 4 fold increase in tDA) at pH 7.8 relative to pH 8.1. This higher
431 particulate DA content, was in the latter study associated with the lowest growth rate found at this
432 low pH level and may hence be explained by a slow-down of cell division and hence
433 accumulation of particulate DA in the cells.

434 With respect to natural assemblage experiments, Tatter et al.(2018) found that particulate DA
435 contents increased at lower pH levels (380 vs. 800 ppm CO₂ corresponding to pH 8.22 and 7.95,
436 respectively) for *P. multiseriis* cells grown with nitrate as N-source at 19°C, but the exact
437 opposite was found when grown with urea as N-source, and no increases or decreases in DA were
438 found when grown at a higher temperature (23°C). Several factors are thus interacting an
439 affecting DA-production, making final conclusions difficult. More recently, during a mesocosm
440 study, Wohlrab et al. (2020) showed that volumetric DA concentrations increased significantly at
441 higher pCO₂/low pH level (1000 µatm ~ pH 7.66) when inorganic macronutrients (N, P and Si)
442 and diatom abundance were limited at the end of the experiment. The authors suggested that
443 when primary metabolism is decreased by nutrient depletion while photosynthesis persists, the
444 available excess energy/ precursors are favored for the production of secondary metabolites e.g.
445 DA production (Bates et al., 1991; Terseleer et al., 2013; Wohlrab et al., 2020).

446 Another possible explanation for an increase in DA at lower pH (as also observed at pH 7.40 for
447 strain IFR-PAU-17) may result from the physiological stress caused by lowering pH levels below

448 adequate pH conditions, e.g. from changes in cellular enzymatic processes, changes in metal
449 speciation, bacterial community composition shifts, nutrient depletion or modifications in the
450 internal optimum pH for DA production, all factors which have been suggested to affect the
451 production of DA (Lundholm et al. 2004; Tatters et al. 2012).

452 Nutrient depletion was not detected in the present study. The decrease in DA content with
453 decreasing pH that we observed in the present study in contrast to previous studies can be
454 explained by some of the same mechanisms as above but with opposite results for different
455 species. It can on the other hand also be explained by cells being under stress and hence
456 allocating less energy for DA production, and more for maintaining growth and homeostasis. The
457 direct effects of changes in environmental pH on DA content is thus unclear but several studies
458 have suggested that it can be related to the changes in intracellular pH and membrane potential, as
459 well as enzyme activity, all of which could influence cell metabolism (Lundholm et al., 2004;
460 Beardal and Raven, 2004; Giordano et al., 2005; Trimborn et al., 2008).

461 The particulate DA content of the two subclones (L3-30 and L3-100) showed similar patterns at
462 the three different pH treatments, but with much lower DA content in L3-30 (e.g. 77% lower at
463 pH 8.07). This variability in DA content may be attributed to the differences in growth rate,
464 assuming that the DA production rates are the same in the two subclones. The faster growing
465 clone, L3-30, had a lower DA content because of DA “dilution” in the cells caused by a faster
466 cell division.

467 The variability in toxin content among the *P. australis* strains seen in the present study
468 emphasizes the difficulties in comparing results from different studies using different strains, and

469 in deriving conclusions about physiological behavior like toxin production and growth response
470 using a single strain. Many physiological studies are still performed based on only one strain,
471 most likely because use of multiple strains multiplies the experimental effort and restricts
472 exploring multiple factors.

473 **1.5 Conclusion**

474 Overall, *P. fraudulenta* and most of *P. australis* strains showed capacity to acclimate and exhibit
475 similar growth rates when comparing current pH (8.07) and projected pH in 2100 (7.80),
476 indicating that these strains may not be affected by ongoing ocean acidification, although daily
477 pH variations due to photosynthesis and respiration processes should be considered, especially as
478 a further decrease in pH (7.40) resulted in a significant reduction in the growth rate of most of *P.*
479 *australis* strains. OA will “demand” that the cells are able to cope with even larger variations in
480 future water pH, as pH will change from a low OA-induced pH to a high pH during bloom
481 periods.

482 For most of the *P. australis* strains, DA content was highest in cultures acclimated at the ambient
483 pH (8.07), and lowest at the projected 2100 seawater pH (7.77). This was however in contrast to
484 most other studies, and thus makes it difficult to predict whether toxicity of *P. auatralis* will
485 present a lower or a higher risk for DA accumulation in a future affected by OA.

486 The diversity in the physiological responses highlights a strong inter- and intra-specific variation
487 in *Pseudo-nitzschia*, and suggests use of multiple strains in future studies. Furthermore, it
488 highlights that the culturing history (e.g. effect of different light intensities) of strains may affect

489 the physiology, an issue that needs future attention, as it may affect deductions from laboratory
490 studies to field scenarios.

491 **Acknowledgements**

492 The authors acknowledge Ifremer and the Regional Council of the “*Région des Pays de la Loire*”
493 for the PhD funding of Nour Ayache. The authors would like to thank Audrey Duval and Nicolas
494 Chomérat from Ifremer, Concarneau, France for providing and identifying the French *Pseudo-*
495 *nitzschia australis* IFR-PAU-17 strain, and Deon Louw and Cecilie Hedemand for providing the
496 Namibian *Pseudo-nitzschia australis* L3-100, L3.4 and L3-30 strains. Thanks are also due to
497 Juliette Fauchot from UMR BOREA, Normandy University, France, for providing the two *P.*
498 *fraudulenta* strains PNfra167 and PNfra169. The authors thank Georges-Augustin Rovillon for
499 his invaluable help for technical assistance in toxin analysis.

500 **References**

- 501 Auro, M.E., Cochlan, W.P., 2013. Nitrogen Utilization and Toxin Production by Two Diatoms of
502 the Pseudo-nitzschia pseudodelicatissima Complex: *P. cuspidata* and *P. fryxelliana*. *J.*
503 *Phycol.* 49, 156–169. <https://doi.org/10.1111/jpy.12033>
- 504 Ayache, N., Hervé, F., Martin-Jézéquel, V., Amzil, Z., Caruana, A.M.N., 2019. Influence of
505 sudden salinity variation on the physiology and domoic acid production by two strains of
506 Pseudo-nitzschia australis. *J. Phycol.* 195, 186–195. <https://doi.org/10.1111/jpy.12801>
- 507 Banse, K., 1976. Algal cell size and the maximum density and biomass of phytoplankton.
508 *Limnol. Oceanogr.* 32, 983–986.
- 509 Bates, S.S., de Freitas, A.S.W., Miley, J.E., Pocklington, R., Quilliam, M.A., Smith, J.C., Worms,
510 J., 1991. Controls on domoic acid production by the diatom *Nitzschia pungens* f. *multiseries*
511 in culture: nutrients and irradiance. *Can. J. Fish. Aquat. Sci.* 48, 1136–44.
- 512 Bates, S.S., Hubbard, K.A., Lundholm, N., Montresor, M., Leaw, C.P., 2018. Pseudo-nitzschia,
513 Nitzschia, and domoic acid: New research since 2011. *Harmful Algae* 79, 3–43.
514 <https://doi.org/10.1016/j.hal.2018.06.001>
- 515 Beardal, J., Raven, J., 2004. The potential effects of global climate change on microalgal
516 photosynthesis, growth and ecology. *Phycologia* 43, 26–40.
- 517 Berge, T., Daugbjerg, N., Andersen, B.B., Hansen, P.J., 2010. Effect of lowered pH on marine
518 phytoplankton growth rates. *Mar. Ecol. Prog. Ser.* 416, 79–91.
519 <https://doi.org/10.3354/meps08780>
- 520 Caldeira, K., Wickett, M.E., 2003. Anthropogenic carbon and ocean pH. *Nature* 425, 365.
521 <https://doi.org/10.1038/425365a>
- 522 Calu, G., 2011. Contribution to the study of Pseudo-nitzschia toxicity: regulation of domoic acid
523 production and synthesis of chemical analogues. Nantes, France.
- 524 Cho, E.S., Kotaki, Y., Park, J.G., 2001. The comparaison between toxic Pseudo-nitzschia
525 multiseries (Hasle) Hasle and non-toxic *P. pungens* (Grunow) Hasle isolated from Jinhae
526 Bay, Korea. *Algae* 16, 275–285.
- 527 Cornwall, C.E., Hepburn, C.D., McGraw, C.M., Currie, K.I., Pilditch, C.A., Hunter, K.A., Boyd,
528 P.W., Hurd, C.L., 2013. Diurnal fluctuations in seawater pH influence the response of a
529 calcifying macroalga to ocean acidification. *Proceedings. Biol. Sci.* 280, 20132201.
530 <https://doi.org/10.1098/rspb.2013.2201>
- 531 Davidson, A.T., McKinlay, J., Westwood, K., Thomson, P.G., Van Den Enden, R., De Salas, M.,
532 Wright, S., Johnson, R., Berry, K., 2016. Enhanced CO₂ concentrations change the structure
533 of Antarctic marine microbial communities. *Mar. Ecol. Prog. Ser.* 552, 93–113.
534 <https://doi.org/10.3354/meps11742>
- 535 Di Liberto, T., 2015. California closes Dungeness and razor clam fisheries due to algal toxin

- 536 [WWW Document]. NOAA Clim. URL <https://www.climate.gov/news-features/event-tracker/california-closes-dungeness-and-razor-clam-fisheries-due-algal-toxin> (accessed
537 5.18.20).
538
- 539 Dickson, A.G., Millero, F.J., 1987. A comparison of the equilibrium constants for the dissociation
540 of carbonic acid in seawater media. *Deep Sea Res. Part A, Oceanogr. Res. Pap.* 34, 1733–
541 1743. [https://doi.org/10.1016/0198-0149\(87\)90021-5](https://doi.org/10.1016/0198-0149(87)90021-5)
- 542 Doney, S.C., 2010. The growing human footprint on coastal and open-ocean biogeochemistry.
543 *Science* (80-.). 328, 1512–1513. [https://doi.org/10.1016/S0140-6736\(16\)32143-2](https://doi.org/10.1016/S0140-6736(16)32143-2)
- 544 Feely, R.A., Sabine, C.L., Hernandez-ayon, J.M., Ianson, D., Hales, B., 2008. Evidence for
545 Upwelling of Corrosive Continental “Acidified” water onto the continental Shelf. *Science*
546 (80-.). 1490, 1–4. <https://doi.org/10.1126/science.1155676>
- 547 Flynn, K.J., Blackford, J.C., Baird, M.E., Raven, J.A., Clark, D.R., Beardall, J., Brownlee, C.,
548 Fabian, H., Wheeler, G.L., 2012. Changes in pH at the exterior surface of plankton with
549 ocean acidification. *Nat. Clim. Chang.* 2, 510–513. <https://doi.org/10.1038/nclimate1489>
- 550 Flynn, K.J., Clark, D.R., Mitra, A., Fabian, H., Hansen, P.J., Glibert, P.M., Wheeler, G.L.,
551 Stoecke, D.K., Blackford, J.C., Brownlee, C., 2015. Ocean acidification with
552 (de)eutrophication will alter future phytoplankton growth and succession. *Proc. R. Soc. B*
553 *Biol. Sci.* 282, 2–7. <https://doi.org/10.1098/rspb.2014.2604>
- 554 Gattuso, J.-P., Hansson, L., 2009. Ocean acidification : background and history, in: Gattuso, J.-P.,
555 Hansson, L. (Eds.), *Ocean Acidification*. pp. 1–20.
- 556 Goldstein, T., Mazet, J.A.K., Zabka, T.S., Langlois, G., Colegrove, K.M., Silver, M., Bargu, S.,
557 Van Dolah, F., Leighfield, T., Conrad, P.A., Barakos, J., Williams, D.C., Dennison, S.,
558 Haulena, M., Gulland, F.M.D., 2008. Novel symptomatology and changing epidemiology of
559 domoic acid toxicosis in California sea lions (*Zalophus californianus*): An increasing risk to
560 marine mammal health. *Proc. R. Soc. B Biol. Sci.* 275, 267–276.
561 <https://doi.org/10.1098/rspb.2007.1221>
- 562 Graneli, E., Haraldsson, C., 1993. Can increased leaching of trace-metals from acidified areas
563 influence phytoplankton growth in coastal waters. *Ambio* 22, 308–311.
- 564 Guillard, R.R.L., 1973. Methods for microflagellates and nanno- plankton, in: Stein, J. (Ed.),
565 *Handbook of Phycological Methods. Culture Methods and Growth Measurements*.
566 Cambridge University Press, New York, pp. 289–312.
- 567 Guillard, R.R.L., Hargraves, P.E., 1993. *Stichochrysis immobilis* is a diatom, not a chrysophyte.
568 *Phycologia* 32, 234–236. <https://doi.org/10.2216/i0031-8884-32-3-234.1>
- 569 Hancock, A.M., Davidson, A.T., Mckinlay, J., Mcminn, A., Schulz, K.G., Van Den Enden, R.L.,
570 2018. Ocean acidification changes the structure of an Antarctic coastal protistan community.
571 *Biogeosciences* 15, 2393–2410. <https://doi.org/10.5194/bg-15-2393-2018>
- 572 Hansen, H.P., Koroleff, F., 1999. Determination of nutrients, in: Grasshoff, K., Kremling, K.,

- 573 Ehrhardt, M. (Eds.), *Methods of Seawater Analysis*, Third Edition. Verlag Chemie,
574 Germany, pp. 159–228.
- 575 Hansen, J., Sato, M., Kharecha, P., Russell, G., Lea, D.W., Siddall, M., 2007. Climate change and
576 trace gases. *Philos. Trans. R. Soc.* 365, 1925–1954. <https://doi.org/10.1098/rsta.2007.2052>
- 577 Hein, M., Sand-Jensen, K., 1997. CO₂ increases oceanic primary production [6]. *Nature*.
578 <https://doi.org/10.1038/41457>
- 579 Hopkinson, B.M., Xu, Y., Shi, D., McGinn, P.J., Morel, F.M.M., 2010. The effect of CO₂ on the
580 photosynthetic physiology of phytoplankton in the Gulf of Alaska. *Limnol. Oceanogr.* 55,
581 2011–2024. <https://doi.org/10.4319/lo.2010.55.5.2011>
- 582 Hutchins, D., Mulholland, M., Fu, F., 2009. Nutrient cycles and marine microbes in a CO₂-
583 enriched ocean. *Oceanography* 22, 128–145. <https://doi.org/10.5670/oceanog.2009.103>
- 584 IPCC, 2014. International Governmental Panel on Climate Change (IPCC), Synthesis Report.
585 Contribution of Working Groups I, II and III to the Fifth Assessment Report of the
586 Intergovernmental Panel on Climate Change. R.K. Pachauri and L.A. Meyer, Geneva,
587 Switzerland.
- 588 Kroeker, K.J., Kordas, R.L., Crim, R., Hendriks, I.E., Ramajo, L., Singh, G.S., Duarte, C.M.,
589 Gattuso, J.P., 2013. Impacts of ocean acidification on marine organisms: Quantifying
590 sensitivities and interaction with warming. *Glob. Chang. Biol.* 19, 1884–1896.
591 <https://doi.org/10.1111/gcb.12179>
- 592 Le Quéré, C., Andrew, R.M., Friedlingstein, P., Sitch, S., Pongratz, J., Manning, A.C.,
593 Korsbakken, J.I., Peters, G.P., Canadell, J.G., Jackson, R.B., Boden, T.A., Tans, P.P.,
594 Andrews, O.D., Arora, V.K., Bakker, D.C.E., Barbero, L., Becker, M., Betts, R.A., Bopp,
595 L., Chevallier, F., Chini, L.P., Ciais, P., Cosca, C.E., Cross, J., Currie, K., Gasser, T., Harris,
596 I., Hauck, J., Haverd, V., Houghton, R.A., Hunt, C.W., Hurtt, G., Ilyina, T., Jain, A.K.,
597 Kato, E., Kautz, M., Keeling, R.F., Klein Goldewijk, K., Körtzinger, A., Landschützer, P.,
598 Lefèvre, N., Lenton, A., Lienert, S., Lima, I., Lombardozzi, D., Metzl, N., Millero, F.,
599 Monteiro, P.M.S., Munro, D.R., Nabel, J.E.M.S., Nakaoka, S.-I., Nojiri, Y., Padin, X.A.,
600 Pregon, A., Pfeil, B., Pierrot, D., Poulter, B., Rehder, G., Reimer, J., Rödenbeck, C.,
601 Schwinger, J., Séférian, R., Skjelvan, I., Stocker, B.D., Tian, H., Tilbrook, B., Tubiello,
602 F.N., Van Der Laan-Luijkx, I.T., Van Der Werf, G.R., Van Heuven, S., Viovy, N.,
603 Vuichard, N., Walker, A.P., Watson, A.J., Wiltshire, A.J., Zaehle, S., Zhu, D., 2018. Global
604 carbon budget 2017. *Earth Syst. Sci. Data* 10, 405–448. <https://doi.org/10.5194/essd-10-405-2018>
- 606 Lefebvre, K.A., Frame, E.R., Kendrick, P.S., 2012. Domoic acid and fish behavior: A review.
607 *Harmful Algae* 13, 126–130. <https://doi.org/10.1016/j.hal.2011.09.011>
- 608 Lewis, E., Wallace, D.W.R., 1998. Program developed for CO₂ system calculations,
609 ORNL/CDIAC-105, Carbon Dioxide Information Analysis Center. Oak Ridge, Tennessee.
610 <https://doi.org/4735>

- 611 Lundholm, N., Hansen, P.J., Kotaki, Y., 2004. Effect of pH on growth and domoic acid
612 production by potentially toxic diatoms of the genera *Pseudo-nitzschia* and *Nitzschia*. *Mar.*
613 *Ecol. Prog. Ser.* 273, 1–15. <https://doi.org/10.3354/meps273001>
- 614 MacIntyre, H.L., Cullen, J.J., 2005. Using cultures to investigate the physiological ecology of
615 microalgae, in: Andersen, R.A. (Ed.), *Algal Culturing Techniques*. Elsevier academic press,
616 Burlington, MA, USA, pp. 287–326.
- 617 Malviya, S., Scalco, E., Audic, S., Vincent, F., Veluchamy, A., Poulain, J., Wincker, P., Iudicone,
618 D., de Vargas, C., Bittner, L., Zingone, A., Bowler, C., 2016. Insights into global diatom
619 distribution and diversity in the world’s ocean. *Proc. Natl. Acad. Sci. U. S. A.* 113, 1516–
620 1525. <https://doi.org/10.1073/pnas.1509523113>
- 621 Mann, D.G., 1988. Why didn’t Lund see sex in *Asterionella*? A discussion of the diatom life
622 cycle in nature, in: Round, F. (Ed.), *Biopress*. Bristol, pp. 385–412.
- 623 McCabe, R.M., Hickey, B.M., Kudela, R.M., Lefebvre, K.A., Adams, N.G., Bill, B.D., Gulland,
624 F.M.D., Thomson, R.E., Cochlan, W.P., Trainer, V.L., 2016. An unprecedented coastwide
625 toxic algal bloom linked to anomalous ocean conditions. *Geophys. Res. Lett.* 43, 10,366–
626 10,376. <https://doi.org/10.1002/2016GL070023>
- 627 McMinn, A., Muller, M.N., Mertin, A., Ryan, K.G., 2014. The Response of antarctic sea ice
628 algae to changes in pH and CO₂. *PLoS One* 9, e86984. <https://doi.org/10.1371/Citation>
- 629 Mehrbach, C., Culbertson, C.H., Hawley, J.E., Pytkowicz, R.M., 1973. Measurement of the
630 apparent dissociation constants of carbonic acid in seawater at atmospheric pressure.
631 *Limnol. Oceanogr.* 18, 897–907. <https://doi.org/10.4319/lo.1973.18.6.0897>
- 632 Middelboe, A.L., Hansen, P.J., 2007. High pH in shallow water macroalgal habitats. *Mar. Ecol.*
633 *Prog. Ser.* 338, 107–117. <https://doi.org/10.2307/24871746>
- 634 Nielsen, L.T., Lundholm, N., Hansen, P.J., 2007. Does irradiance influence the tolerance of
635 marine phytoplankton to high pH? *Mar. Biol. Res.* 3, 446–453.
636 <https://doi.org/10.1080/17451000701711820>
- 637 Orr, J.C., Fabry, V.J., Aumont, O., Bopp, L., Doney, S.C., Feely, R.A., Gnanadesikan, A.,
638 Gruber, N., Ishida, A., Joos, F., Key, R.M., Lindsay, K., Maier-Reimer, E., Matear, R.,
639 Monfray, P., Mouchet, A., Najjar, R.G., Plattner, G.K., Rodgers, K.B., Sabine, C.L.,
640 Sarmiento, J.L., Schlitzer, R., Slater, R.D., Totterdell, I.J., Weirig, M.F., Yamanaka, Y.,
641 Yool, A., 2005. Anthropogenic ocean acidification over the twenty-first century and its
642 impact on calcifying organisms. *Nature* 437, 681–686. <https://doi.org/10.1038/nature04095>
- 643 Pan, Y., Subba Rao, D. V., Mann, K.H., 1996. Acclimation to low light intensity in
644 photosynthesis and growth of *Pseudo-nitzschia multiseries* Hasle, a neurotoxic diatom.
645 *J. Plankton Res.* 18, 1427–1438. <https://doi.org/10.1093/plankt/18.8.1427>
- 646 Reinfelder, J.R., 2011. Carbon Concentrating Mechanisms in Eukaryotic Marine Phytoplankton.
647 <https://doi.org/10.1146/annurev-marine-120709-142720>

- 648 Riebesell, U., 2004. Effects of CO₂ enrichment on marine phytoplankton. *J. Oceanogr.* 60, 719–
649 729. <https://doi.org/10.1007/s10872-004-5764-z>
- 650 Riebesell, U., Schulz, K.G., Bellerby, R.G.J., Botros, M., Fritsche, P., Meyerhöfer, M., Neill, C.,
651 Nondal, G., Oschlies, A., Wohlers, J., Zöllner, E., 2007. Enhanced biological carbon
652 consumption in a high CO₂ ocean. *Nature* 450, 545–548.
653 <https://doi.org/10.1038/nature06267>
- 654 Rost, B., Zondervan, I., Wolf-Gladrow, D., 2008. Sensitivity of phytoplankton to future changes
655 in ocean carbonate chemistry: current knowledge, contradictions and research directions.
656 *Mar. Ecol. Prog. Ser.* 373, 227–237. <https://doi.org/10.3354/meps07776>
- 657 Schippers, P., Lürling, M., Scheffer, M., 2004a. Increase of atmospheric CO₂ promotes
658 phytoplankton productivity. *Ecol. Lett.* 7, 446–451. <https://doi.org/10.1111/j.1461-0248.2004.00597.x>
- 660 Schippers, P., Lürling, M., Scheffer, M., 2004b. Increase of atmospheric CO₂ promotes
661 phytoplankton productivity. *Ecol. Lett.* 7, 446–451. <https://doi.org/10.1111/j.1461-0248.2004.00597.x>
- 663 Scholin, C.A., Gulland, F., Doucette, G.J., Benson, S., Busman, M., Chavez, F.P., Cordaro, J.,
664 DeLong, R., De Vogelaere, A., Harvey, J., Haulena, M., Lefebvre, K., Lipscomb, T.,
665 Loscutoff, S., Lowenstine, L.J., Marin, R., Miller, P.E., McLellan, W.A., Moeller, P.D.R.,
666 Powell, C.L., Rowles, T., Silvagni, P., Silver, M., Spraker, T., Trainer, V., Van Dolah, F.M.,
667 2000. Mortality of sea lions along the central California coast linked to a toxic diatom
668 bloom. *Nature* 403, 80–84. <https://doi.org/10.1038/47481>
- 669 Sobrinho, B.F., De Camargo, L.M., Sandrini-Neto, L., Kleemann, C.R., Da Costa Machado, E.,
670 Mafra, L.L., 2017. Growth, toxin production and allelopathic effects of *Pseudo-Nitzschia*
671 *multiseriis* under Iron-enriched conditions. *Mar. Drugs* 15, 331.
672 <https://doi.org/10.3390/md15100331>
- 673 Solorzano, L., Sharp, J.H., 1980. Determination of total dissolved nitrogen in natural waters.
674 *Limnol. Oceanogr.* 25, 751–754.
- 675 Sun, J., Hutchins, D.A., Feng, Y., Seubert, E.L., Caron, D.A., Fu, F.X., 2011. Effects of changing
676 pCO₂ and phosphate availability on domoic acid production and physiology of the marine
677 harmful bloom diatom *Pseudo-nitzschia multiseriis*. *Limnol. Oceanogr.* 56, 829–840.
678 <https://doi.org/10.4319/lo.2011.56.3.0829>
- 679 Tatters, A.O., Fu, F.-X., Hutchins, D.A., 2012. High CO₂ and silicate limitation synergistically
680 increase the toxicity of *Pseudo-nitzschia fraudulenta*. *PLoS One* 7, e32116.
681 <https://doi.org/10.1371/journal.pone.0032116>
- 682 Tatters, A.O., Schnetzer, A., Xu, K., Walworth, N.G., Fu, F., Spackeen, J.L., Sipler, R.E.,
683 Bertrand, E.M., McQuaid, J.B., Allen, A.E., Bronk, D.A., Gao, K., Sun, J., Caron, D.A.,
684 Hutchins, D.A., 2018. Interactive effects of temperature, CO₂ and nitrogen source on a
685 coastal California diatom assemblage. *J. Plankton Res.* 40, 151–164.

- 686 <https://doi.org/10.1093/plankt/fbx074>
- 687 Terseleer, N., Gypens, N., Lancelot, C., 2013. Factors controlling the production of domoic acid
688 by *Pseudo-nitzschia* (Bacillariophyceae): A model study. *Harmful Algae* 24, 45–53.
689 <https://doi.org/10.1016/j.hal.2013.01.004>
- 690 Thorel, M., Fauchot, J., Morelle, J., Raimbault, V., Le Roy, B., Miossec, C., Kientz-Bouchart, V.,
691 Claquin, P., 2014. Interactive effects of irradiance and temperature on growth and domoic
692 acid production of the toxic diatom *Pseudo-nitzschia australis* (Bacillariophyceae). *Harmful*
693 *Algae* 39, 232–241. <https://doi.org/10.1016/J.HAL.2014.07.010>
- 694 Trainer, V.L., Bates, S.S., Lundholm, N., Thessen, A.E., Cochlan, W.P., Adams, N.G., Trick,
695 C.G., 2012. *Pseudo-nitzschia* physiological ecology, phylogeny, toxicity, monitoring and
696 impacts on ecosystem health. *Harmful Algae* 14, 271–300.
697 <https://doi.org/10.1016/j.hal.2011.10.025>
- 698 Trimborn, S., Brenneis, T., Sweet, E., Rost, B., 2013. Sensitivity of Antarctic phytoplankton
699 species to ocean acidification: Growth, carbon acquisition, and species interaction. *Limnol.*
700 *Oceanogr.* 58, 997–1007. <https://doi.org/10.4319/lo.2013.58.3.0997>
- 701 Trimborn, S., Lundholm, N., Thoms, S., Richter, K.U., Krock, B., Hansen, P.J., Rost, B., 2008.
702 Inorganic carbon acquisition in potentially toxic and non-toxic diatoms: The effect of pH-
703 induced changes in seawater carbonate chemistry. *Physiol. Plant.* 133, 92–105.
704 <https://doi.org/10.1111/j.1399-3054.2007.01038.x>
- 705 Wingert, C., 2017. The effects of ocean acidification on growth, photosynthesis, and domoic acid
706 production by the toxigenic diatom, *Pseudo-nitzschia australis*.
- 707 Wohlrab, S., John, U., Klemm, K., Eberlein, T., Forsberg Grivogiannis, A.M., Krock, B.,
708 Frickenhaus, S., Bach, L.T., Rost, B., Riebesell, U., Van de Waal, D.B., 2020. Ocean
709 acidification increases domoic acid contents during a spring to summer succession of coastal
710 phytoplankton. *Harmful Algae* 92, 101697. <https://doi.org/10.1016/j.hal.2019.101697>
- 711 Zhu, Z., Qu, P., Gale, J., Fu, F., Hutchins, D.A., 2017. Individual and interactive effects of
712 warming and CO₂ on *Pseudo-nitzschia subcurvata* and *Phaeocystis antarctica*, two
713 dominant phytoplankton from the Ross Sea, Antarctica. *Biogeosciences* 14, 5281–5295.
714 <https://doi.org/10.5194/bg-14-5281-2017>

715